# Superconductivity without Nesting in LiFeAs

S. V. Borisenko,[1] V. B. Zabolotnyy,[1] D. V. Evtushinsky,[1] T. K. Kim,[1] I. V. Morozov,[1,2] A. N. Yaresko,[3] A. A. Kordyuk,[1] G. Behr,[1] A. Vasiliev,[2] R. Follath,[4] and B. Büchner[1]

[1]*Leibniz-Institute for Solid State Research, IFW-Dresden, D-01171 Dresden, Germany*
[2]*Moscow State University, Moscow 119991, Russia*
[3]*Max-Planck-Institute for Solid State Research, D-70569 Stuttgart, Germany*
[4]*Helmholtz-Zentrum Berlin, BESSY, D-12489 Berlin, Germany*

(Received 26 February 2010; published 2 August 2010)

We have studied the electronic structure of the nonmagnetic LiFeAs ($T_c \sim 18$ K) superconductor using angle-resolved photoemission spectroscopy. We find a notable absence of the Fermi surface nesting, strong renormalization of the conduction bands by a factor of 3, high density of states at the Fermi level caused by a van Hove singularity, and no evidence for either a static or a fluctuating order except superconductivity with in-plane isotropic energy gaps. Our observations suggest that these electronic properties capture the majority of ingredients necessary for the superconductivity in iron pnictides.

DOI: 10.1103/PhysRevLett.105.067002 PACS numbers: 74.70.Xa

The synthesis of another iron superconductor has immediately attracted much attention already for several reasons [1–3]. LiFeAs is one of the few superconductors which does not require additional charge carriers and is characterized by $T_c$ approaching the boiling point of hydrogen. Similar to $AeFe_2As_2$ (122) and LnOFeAs (1111) parent compounds, LiFeAs consists of nearly identical $(Fe_2As_2)^{2-}$ structural units and all three are isoelectronic, though the former do not superconduct. The band structure calculations unanimously yield the same shapes of the Fermi surfaces (FS), very similar densities of states, and low energy electronic dispersions ([4,5], and the supplementary material [6]) and even find in LiFeAs an energetically favorable magnetic solution which exactly corresponds to the famous stripelike antiferromagnetic order in 122 and 1111 systems [5,7,8]. The experiments, however, show a rather different picture. The structural transition peculiar to 122 and 1111 families is remarkably absent in LiFeAs and is not observed under applied pressure of up to 20 GPa [9,10]. Resistivity and susceptibility as well as $\mu$-spin rotation experiments show no evidence for the magnetic transition [11,12]. Only a weak magnetic background [12] and field induced magnetism in the doped compound have been detected [11]. It is therefore not clear why the isoelectronic and nearly isostructural FeAs blocks induce fundamentally different physical properties of the material. In this Letter we suggest that this occurs due to the important distinctions in the electronic structure and single out those which seem to be indispensable for the superconductivity.

The knowledge gained from angle-resolved photoemission (ARPES) experiments on Fe pnictides has often been questioned because of the possible influence of the polar surface inevitably exposed by the cleavage of 122 and 1111 single crystals. LiFeAs offers a unique opportunity to overcome this difficulty since the cleavage occurs between the two layers of Li atoms resulting in equivalent and neutral counterparts. Further details on the ARPES experiment, crystal growth, and band structure calculations are given [6].

In Fig. 1(a) we show the Fermi surface map of LiFeAs which is the momentum distribution of the photoemission intensity integrated within the narrow energy interval around the Fermi level. Three clear features are visible on the map: a high-intensity butterflylike shape at the $\Gamma$ point, a well-defined barrel-like FS also centered at $\Gamma$, and a double-walled structure with somewhat obscure contours around the $M$ point. Momentum-energy cuts along the selected directions passing near $M$ and $\Gamma$ points and marked in panel (a) by white dashed lines are presented in Figs. 1(b) and 1(c). While both dispersive features in Fig. 1(b) as well as the leftmost one in Fig. 1(c) clearly cross the Fermi level thus supporting a double-walled electronlike FS around $M$ and large holelike FS around $\Gamma$, respectively, the other two features from Fig. 1(c) only come close to the Fermi level without clear crossing, at least for the given cut through the momentum space. We have found that for certain excitation energies these features do cross the Fermi level resulting in very small holelike FSs, thus completing the analogy with the FS topolgy of 122 and 1111 systems: there are in total five FSs supported by five bands. The sketch in Fig. 1(a) schematically shows all FS features centered in one point to facilitate the comparison of their sizes. The striking peculiarity of this FS shape is the absolute absence of the $(\pi, \pi)$ nesting peculiar to other pnictides.

According to the existent band structure calculations, including our own study (see [6]), the FS of LiFeAs also consists of three holelike FSs around the $\Gamma$ point and two electronlike ones at the corner of the Brillouin zone. In Fig. 2 we compare our experimental data with the calculations. Three FS maps shown in Figs. 2(a)–2(c) are recorded at different photon energies which correspond to different $k_z$ values and thus should reflect the variations of

 

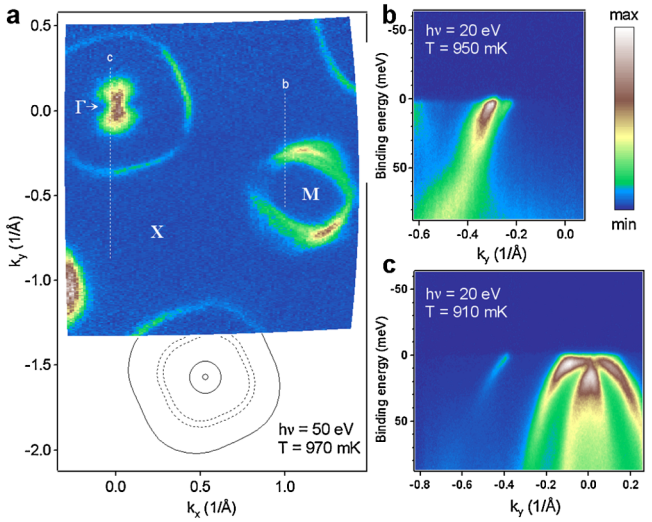


FIG. 1 (color online). Fermi surface shape and topology. (a) Momentum distribution map of the photoemission intensity integrated within 5 meV around the Fermi level. Solid black lines represent Γ—centered Fermi contours, dashed lines—most pronounced $M$-centered Fermi contours. (b),(c) Momentum-energy cuts along the vertical directions marked by the white dashed lines in panel (a).

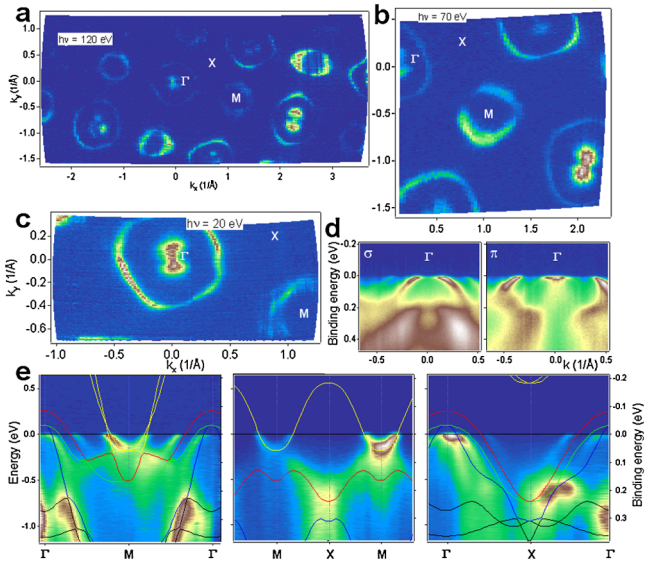


FIG. 2 (color online). Comparison with the LDA calculations. (a)–(c) Fermi surface maps taken at different excitation energies at $T \sim 1$ K. (d) Momentum-energy cut through the Γ point measured with the $\sigma$ (left) and $\pi$ (right) polarizations. Photon energy is 67 eV. (e) High-symmetry momentum-energy cuts together with the results of the band structure calculations.

the FS with $k_z$. Indeed, being well defined and having the same size in all maps, the largest Γ barrel is nearly ideally two-dimensional in close agreement with the calculations. At the same time the degree of three dimensionality of the two small Γ- centered FSs seems to be less pronounced in the experiment. The distribution of the spectral weight around the $M$ point is photon energy dependent and takes the shape of either crossed ellipses or rounded squares or displays the signatures of both [see also Fig. 1(a)], more or less exactly following the theoretical predictions.

To understand in more detail the butterflylike intensity spot at Γ, which universally appears in all maps and looks different only in replicated Γ points at nonzero momentum, we performed the polarization dependent measurements. The strong influence of the matrix elements on the photoemission intensity seen in Fig. 2(d) is expected and fully explainable in terms of symmetry composition of the states forming two small FSs at Γ point. According to calculations [6] these states are formed by $d_{xz}$ ($d_{yz}$) orbitals and are therefore enhanced (suppressed) when probed in $\pi(\sigma)$ polarization geometries [13]. Note that the behavior of the outer Γ barrel is also easy to understand, as it is formed by the states having $d_{x^2-y^2}$ symmetry and thus also sensitive to such a variation of the geometry of the experiment. From Fig. 2(d) [see also Fig. 1(c)] it also follows that the tops of both bands practically touch the Fermi level with the top of the larger one having an extended flat shape. This results in an anomalous enhancement of the density of states at the Fermi level.

Knowledge of the FS shape and topology allowed us to estimate the number of charge carriers in the system. Neglecting the contribution of the smallest Γ-FS it turns out that two electronlike pockets compensate two holelike Γ-FSs and the total occupation of the corresponding four bands roughly equals four electrons. More rigorous estimates which take into account $k_Z$ dispersion of the electron pockets also give the stoichiometric solution within the error bars. The measurements have been carried out on three different single crystals and yielded reproducible results, thus indicating the absence of noticeable Li content variations (see [6]).

In Fig. 2(e) we compare directly the calculated band structure and experimental data along the high-symmetry directions. We made a tight-binding fit to the best defined experimental band which supports the large Γ barrel and found a remarkable qualitative agreement with the $d_{x^2-y^2}$ originated band from the local-density approximation (LDA) calculations. The ratio of the bandwidths turned out to be equal to 3.1 (1 eV vs 0.326 eV). We then applied this renormalization factor to bring the experimental data and the calculated bands to the same energy scale. Overall agreement is very reasonable, taking into account that we have identified all bands in the vicinity of the Fermi level and associated them with the corresponding features in the ARPES spectra. Note that the electronlike pocket at $M$ formed by another band is satisfactorily reproduced as well. As seen from the figure and confirmed by the calculations, a selective shift of the $d_{x^2-y^2}$ band by 150 meV perfectly reproduces the shape of the large holelike Fermi surface and dispersion over the whole bandwidth.

This agreement together with the extremely low temperatures at which we carried out our experiments clearly speaks in favor of a nonmagnetic ground state realized in

LiFeAs. This is supported by the fact that having explored the large portions of the $k$ space at different experimental conditions, we have not found any typical spectroscopic signatures of commensurate or incommensurate ordering appearing in a form of replica due to Fermi surface reconstruction or suppressed spectral weight due to gap, etc. [14,15]. What is not captured by the LDA approach, which predicts magnetism in LiFeAs [5,7], are the actual absence of nesting and renormalization by the factor of ~3. The energy gain from the opening of the gaps at or near the Fermi level due to the FS reconstruction is obviously more significant in a system with 3 times narrower bandwidth. That is probably why the spin-density wave (SDW) order does not disappear immediately upon doping in 122 and 1111 families of Fe pnictides. In LiFeAs, where the ($\pi$, $\pi$) nesting is absent, static magnetism disappears completely. Our results thus strongly imply the decisive role of nesting in the formation of SDW.

The ultralow temperature of our measurements made it possible to study the symmetry of the superconducting order parameter of LiFeAs close to the ground state. We have clearly observed the opening of the superconducting gap in all $k_F$ points with the onset at the nominal $T_c$ of ~18 K. A typical example is presented in Fig. 3(a) where the crossing of the FS at point $A$ [see Fig. 3(d)] is shown for two temperatures, above and below the transition. Upon entering the superconducting state, the usual BCS-like bending back of the dispersive feature is apparently seen in the lower panel and the experimental dispersion, determined as a set of maxima of the momentum distribution curves, exhibits peculiar transformation from the straight line to the "$S$"-shaped curve in the immediate vicinity of the Fermi level (not shown). This is accompanied by the depletion of the spectral weight at the Fermi level with concomitant shift of the leading-edge midpoint of the $k_F$-EDC as seen in Fig. 3(b) and in zoomed version in Fig. 3(c). In passing, there are well-defined quasiparticle excitations, both above and below $T_c$ [Fig. 3(b)] as well as characteristic "kinks" in the dispersion at 18, 30, and 43 meV [16]. We conclude the presentation of the experimental material by plotting the kinetic energies of the leading-edge midpoints as a function of momentum in Fig. 3(d). The typical size of the leading-edge gap of the holelike FSs is estimated to be ~1.5–2.5 meV, while for the electronlike FSs we observed slightly larger values of ~2–3.5 meV implying a multiband superconductivity in LiFeAs. In both cases, as follows from Fig. 3(d), the anisotropy of the gap is not dramatic, although taking into account the relatively small absolute values of the gaps, even small variations may be of interest. More rigorous estimates based on accurate fitting including the resolution contribution result in the superconducting gap of 3.2 meV on the electronlike pockets, which is in excellent agreement with the recent small-angle neutron scattering data [17]. Because of peculiar polarization dependent behavior seen in Fig. 2(d) the actual gap size at the $\Gamma$ point is smaller than it is implied by the map of

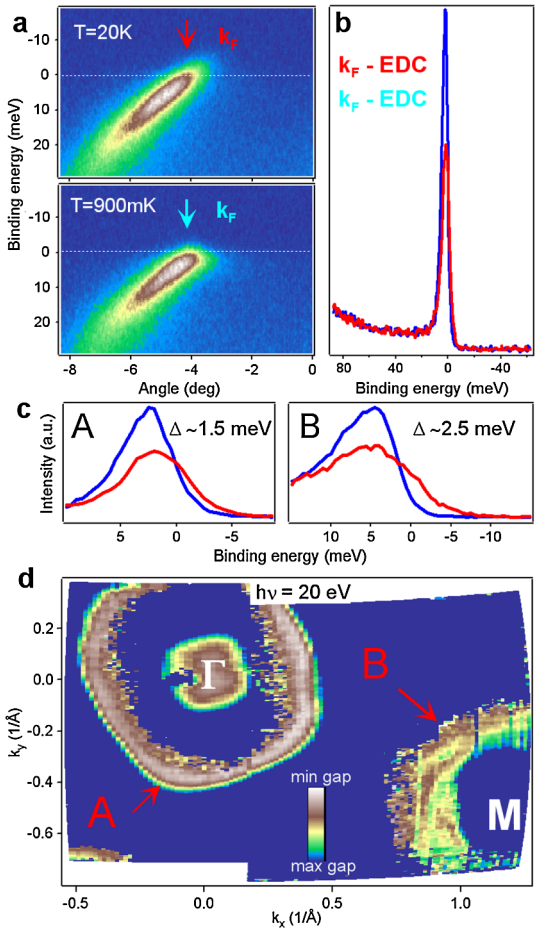


FIG. 3 (color online). Superconductivity in LiFeAs. (a) Fermi surface crossings at the point $A$ [see panel (d)] taken above and below $T_c$(~18 K). (b) Energy distribution curves from panels (a) corresponding to the $k_F$. (c) Energy distribution curves corresponding to Fermi momenta $A$ and $B$ measured above (20 K) and below (900 mK) $T_c$. (d) Kinetic energies of the leading-edge midpoints of all energy distribution curves from the shown momentum space region in the false color scale. The local maxima of this distribution correspond to $k_F$ points also seen in Fig. 2(c) and give a good measure of the superconducting gap.

leading-edge gaps [Fig. 3(d)] and is estimated to be of the order of 1 meV.

Disregarding for a moment any relation to other families of Fe pnictides and thus possible presence of the so far not detected spin fluctuations capable of binding electrons in pairs [18], it is crucial to understand what makes a stoichiometric compound with a plane crystal structure a multiband superconductor with a considerable critical temperature and weakly in-plane anisotropic order parameter. The presented data imply that the only remarkable property of the electronic structure of LiFeAs which makes it so special and intimately connects it to other superconductors such as 2$H$-$NbSe_2$, A15 compounds, $MgB_2$ and the cuprates is the proximity of the van Hove singularity to the Fermi level. In Fig. 4 we suggest a very simple scenario which emphasizes the role of nesting for density wave

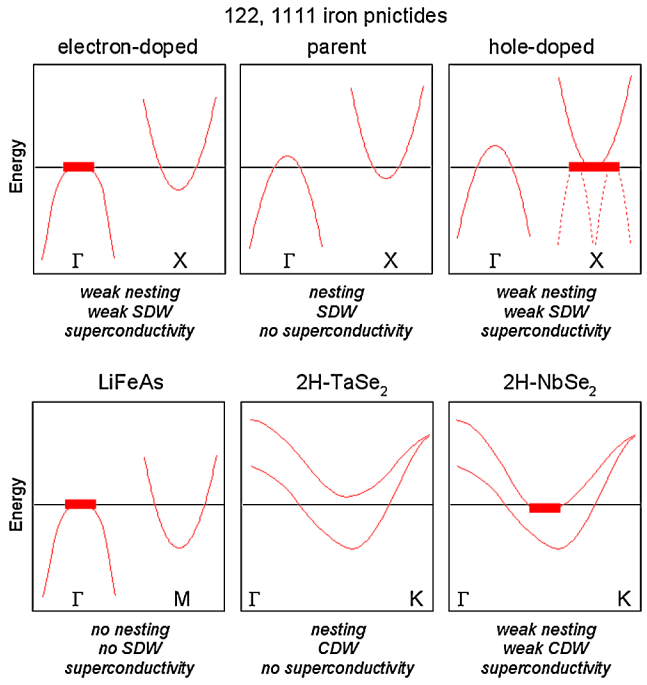


FIG. 4 (color online). van Hove singularities in Fe pnictides and chalcogenides. Schematic illustration of the main features in the electronic structure of the 122 and 1111 pnictides, LiFeAs, $2H$-$TaSe_2$, and $2H$-$NbSe_2$. Curves represent the band dispersions along the high-symmetry directions. Thick lines represent van Hove sigularities, i.e., the flat extrema of the corresponding bands or the saddle point.

orders and van Hove singularities for the superconductivity in pnictides and $2H$-$NbSe_2$. In the parent compounds and in $2H$-$TaSe_2$ the presence of the nesting reconstructs the original Fermi surface and induces the static density wave order resulting in the absence of the superconductivity (or its strong suppression). By doping the holes into the parent pnictide (or substituting Ta by Nb) we destroy the nesting and approach the bottoms of the electronlike bands (or saddle point in $2H$-$NbSe_2$) thus bringing high density of states to the Fermi level. As a consequence, the density wave order is strongly suppressed and superconductivity occurs. The same holds for the electron-doped side of the phase diagram. Now the tops of the holelike bands show up at the Fermi level. In this sense LiFeAs appears to be similar to electron-doped pnictides since in this case the top of the holelike band coincides with the Fermi level already in the pristine compound. It is important to note that merely the extremum of a paraboloidlike band touching the Fermi level will not result in DOS boost at the Fermi level in a two-dimensional material. It has to be either a saddle point or an extended flat region of the dispersion, as is the case in the electronic structures sketched in Fig. 4. The origin of such singularity in LiFeAs and other pnictides remains unclear, though the strong electron-boson coupling close to the Fermi level [16] could play an important role in flattening of the top of the band.

The example of LiFeAs suggests that the intriguing presence of the density waves or their fluctuations in many families of the superconductors may turn out to be rather "technical": they neighbor the superconductivity only because, purely from the topological considerations, the nesting is very probable to occur when tuning the system from one van Hove instability to another by doping in multiband superconductors (see Fig. 4). On the other hand, the nonperfect nesting corresponding to the fading density wave order may result in still larger density of states at the Fermi level thus promoting the superconductivity [19]. However, in view of our present results, the van Hove singularity close to the Fermi level seems to be a necessary condition for the onset of superconductivity, and not only in the pnictides. Apart from this observation, the studied electronic properties clearly indicate that the material itself has a potential of reaching the level comparable to that of BSCCO in the cuprates in terms of its representativeness of the whole family of Fe superconductors.

We acknowledge fruitful discussions with Ernst Bauer, Sergey Bud'ko, Ralf Claessen, Ilya Eremin, Hideo Hosono, Arno Kampf, Dirk van der Marel, Joel Mesot, and Werner Weber. The project was supported, in part, by the DFG under Grants No. KN393/4, BO 1912/2-1, BE1749/13, 486RUS 113/982/0-1 as well as priority program SPP1458. I. V. Morozov also acknowledges support from the Ministry of Science and Education of the Russian Federation under State Contract P-279. We are grateful to S. Graser for sharing with us his results of the band structure calculations.

[1] X. C. Wang *et al.*, Solid State Commun. **148**, 538 (2008).
[2] J. H. Tapp *et al.*, Phys. Rev. B **78**, 060505(R) (2008).
[3] M. J. Pitcher *et al.*, Chem. Commun. (Cambridge) **2008**, 5918 (2008).
[4] I. A. Nekrasov, Z. V. Pchelkina, and M. V. Sadovskii, JETP Lett. **88**, 543 (2008).
[5] D. J. Singh, Phys. Rev. B **78**, 094511 (2008).
[6] See supplementary material at http://link.aps.org/supplemental/10.1103/PhysRevLett.105.067002 for experimental and computational details.
[7] Y. F. Li *et al.*, Eur. Phys. J. B **72**, 153 (2009).
[8] R. A. Jishi and H. M. Alyahyaei, Adv. Condens. Matter Phys. **2010**, 1 (2010).
[9] S. J. Zhang *et al.*, Phys. Rev. B **80**, 014506 (2009).
[10] M. Gooch, *et al.*, Europhys. Lett. **85**, 27005 (2009).
[11] F. L. Pratt *et al.*, Phys. Rev. B **79**, 052508 (2009).
[12] C. W. Chu *et al.*, Physica (Amsterdam) **469C**, 326 (2009).
[13] T. Shimojima *et al.*, Phys. Rev. Lett. **104**, 057002 (2010).
[14] S. V. Borisenko *et al.*, Phys. Rev. Lett. **100**, 196402 (2008).
[15] V. B. Zabolotnyy *et al.*, Europhys. Lett. **86**, 47005 (2009).
[16] A. A. Kordyuk *et al.*, arXiv:1002.3149v2.
[17] D. S. Inosov *et al.*, Phys. Rev. Lett. **104**, 187001 (2010).
[18] T. Dahm *et al.*, Nature Phys. **5**, 217 (2009).
[19] V. B. Zabolotnyy *et al.*, Nature (London) **457**, 569 (2009).